JOURNAL OF MATERIALS SCIENCE 35 (2000) 5047–5055

DSC and TEM investigations on multiple melting phenomena in isotactic polystyrene*

T. LIU, S. YAN, M. BONNET, I. LIEBERWIRTH, K.-D. ROGAUSCH, J. PETERMANN
Institute of Materials Science, Department of Chemical Engineering, University of Dortmund, D-44221 Dortmund, Germany
E-mail: peterman@chemietechnik.uni-dortmund.de

The multiple melting behavior and morphologies of isotactic polystyrene (iPS) isothermally crystallized from the glassy state have been investigated by differential scanning calorimetry (DSC) and transmission electron microscopy (TEM). The combination of thermal analysis and morphological results indicates that two lamellar populations are responsible for the so-called double melting behavior in iPS. The low-temperature melting peak is attributed to the melting of less perfect (thinner or defect containing) subsidiary lamellae formed in the framework of the dominant (thicker or more perfect crystalline) lamellae upon isothermal crystallization. The high-temperature one is mainly due to the melting of the dominant thicker lamellae, and to some less extent, the melting of a recrystallized population coming from the melted defect lamellae during the heating process in DSC.

1. Introduction

Many semicrystalline polymers, such as poly(ether ether ketone) (PEEK), poly(ethylene terephthalate) (PET), poly(phenylene sulfide) (PPS), isotactic polystyrene (iPS), exhibit more than one maximum in the melting endotherms upon scanning in the DSC. Up to date, there are considerable controversies in the literature concerning the origin of the so-called multiple melting behavior, particularly for the low-temperature endotherm, commonly observed for semicrystalline polymers. To our knowledge, the explanations for the origin of the lower melting peak can be approximately grouped into the following models. (i) Melting-recrystallization model [1–6], which advocates that the lower endotherm represents the melting of most of the lamellae initially present, while that at higher temperature represents the melting of thicker and more perfect lamellae formed by recrystallization of partially melted material. (ii) Dual lamellar thickness model [7–12], which suggests that the double endothermic behavior is associated with the melting of lamellae having a bimodal distribution of thickness. The two branches of this model are the dual lamellar stack model [7, 8] and the lamellar insertion model [9–10]. (iii) Different-morphology model [13]. According to Marand and Prasad, the double melting behavior exhibited in PEEK for crystallization temperatures above 300°C can be due to the formation of two morphologies, spherulitic and crystal-aggregate-like structures. (iv) Physical aging model [14], which prefers that the low endotherm is the enthalpic recovery of a physically aged rigid amorphous fraction. (v) Perfect and imperfect crystal model [15, 16]. For instance, the high- and low-melting peaks of poly(aryl ether ketone)s isothermally crystallized from the glassy state is attributed to the perfect and imperfect crystals, respectively. (vi) Different crystal structure model [17], which associates the first melting peak, appearing on linear heating after a period of isothermal crystallization, with chain-folded crystals and the second endotherm with crystals containing some partially extended chains. (vii) "Pseudo-crystalline" phase relaxation model [18], which is recently proposed by our research group. In this model, the lowest endothermic "annealing peak" is ascribed to a relaxation of the "pseudo-crystalline" phase into the relaxed amorphous component. Moreover, some other models, such as disorientation model, crosslinking model, and so on, are also proposed to explain the multiple melting behavior of the semicrystalline polymers.

However, up to the present there exist more or less divergences among these models as mentioned above. No consensus has been reached as to the origin of multiple melting behavior of the semicrystalline polymers. And a model that is reasonably compatible with all physical observations has not yet emerged. Therefore, a complete understanding of the origin of dual or multiple melting behavior (especially of the low-temperature endotherm) is of great significance and should provide a new insight into the crystallization and melting process of crystalline polymers [19]. It is also very likely that more than one reason may be responsible for multiple melting peaks of crystalline polymers.

On the other hand, the extensive studies on multiple melting behavior are mainly focused on the

* Dedicated in memory to Prof. Dr. A. Keller.

melt-crystallized polymer samples, and less attention is paid to the cold-crystallized ones. In addition, the melting process is usually studied on bulk materials by techniques such as calorimetry (DSC), X-ray scattering (WAXS, SAXS), and density measurements. Since these techniques involve the study of bulk samples, normally no direct information can be obtained on the single lamellar level during the melting processes. Nevertheless, at this aspect, the transmission electron microscopy (TEM) technique is a powerful tool, which can provide confirmative evidence. Therefore, a more complete description and understanding on the multiple endothermic behavior of iPS requires confirmation by morphological observations using more direct techniques such as TEM and confirmation by other experimental techniques.

In our present study, we attempt to investigate the complex melting behavior of iPS by combining the TEM technique with the calorimetry method. This polymer is chosen as the studied system based on the following considerations: (1) Characteristic slow overall crystallization rate of iPS makes this polymer an ideal subject for the study and refinement of multiple melting in polymers, due to the possibility of following the crystallization and melting process in the DSC. (2) It has only one crystal modification, which avoids the complexity resulting from the polymorphism phenomena. (3) It is less radiation-sensitive than most other polymers [20], and therefore very suitable for TEM investigations.

2. Experimental

The powdery iPS sample ($M_w = 752000$, isotacticity: 97%) was purchased from Polymer Laboratories. To obtain amorphous samples, pure iPS was heated to 250°C for 5 min, and subsequently quenched into cold water. Then the amorphous samples were isothermally crystallized at 160°C and 180°C for different times, respectively. The reasons, why these two temperatures were selected are as follows: first, at these two temperatures the multiple melting peaks can be well separated from one another; second, the magnitude of the low-temperature melting peak ($T_{m,1}$) is very different at 160°C and 180°C. Therefore, we will present and discuss the results by dividing two parts in the *Results and discussion* section according to these two crystallization temperatures. The originally obtained crystalline samples were subsequently thermally treated (partial melting experiments) at different temperatures for different times for the use of DSC measurements or TEM observations.

DSC experiments were performed in a DSC-2920 from TA Instruments coupled with a TA-2000 control system. The temperature was accurately calibrated with tin, gallium, and indium using standard procedure. All the samples were heated with a scanning rate of 10°C/min. The weights of all the samples were in the range of 5 ± 0.1 mg. All crystallization and melting treatments were performed under nitrogen atmosphere in order to diminish oxidation.

Thin films for direct TEM observation were obtained by the following procedure: firstly, the dilute polymer-xylene solution (with concentration of *ca*. 0.1%-w/v) was dropped onto mica covered with carbon film, then the polymer films with carbon-support film were floated on the water surface and transferred onto electron microscope copper grids, finally the obtained thin films were melted at 250°C for 5 min and quenched into cold water, simulating the procedure of the DSC samples. The samples were investigated using a Philips CM200 TEM operated at 200 kV, and bright-field (BF) electron micrographs were obtained by defocusing the objective lens.

3. Results and discussion

3.1. Investigations on iPS samples cold-crystallized isothermally at 160°C

Fig. 1 shows the DSC trace of iPS cold-crystallized at 160°C for 12 hours. It can be seen, that three endothermic peaks (labelled as T_a, $T_{m,1}$ and $T_{m,2}$ in the order of temperature from low to high) and an exothermic recrystallization peak (labelled as $T_{c,re}$, which is located between the last two melting peaks) are observed. The first endotherm (about 175°C), T_a, is the so-called "annealing peak", whose position is always at *ca.* 10∼15°C above the cold-crystallization or annealing temperature. And the positions of $T_{m,1}$, $T_{c,re}$ and $T_{m,2}$ are observed at about 202°C, 208°C and 222°C, respectively. Almost 30 years ago, Challa and his coworkers [21–23] also observed the triple melting peaks for the melt-crystallized iPS samples. They suggested, that the lowest small endothermic peak (i.e., the "annealing peak"), which was just above the crystallization temperature, was originated from secondary crystallization of the melt trapped within the spherulites. The next melting endotherm was related to the normal primary crystallization process. And the third melting peak came from the second one by continuous melting and recrystallization during the scan. However, our experimental results from TEM do not confirm exactly the melting mechanism proposed by Challa *et al*.

The TEM micrograph and its corresponding electron diffraction pattern of an iPS thin film isothermally cold-crystallized at 160°C for 12 hours is shown in Fig. 2. It

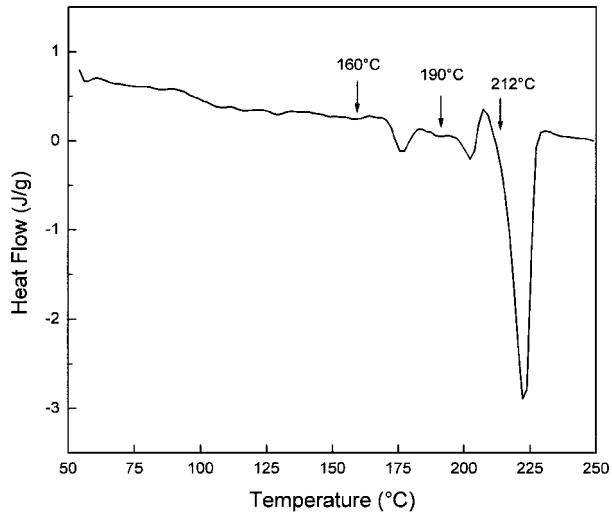

Figure 1 DSC thermogram of iPS isothermally cold-crystallized at 160°C for 12 hours. The heating rate is 10°C/min.

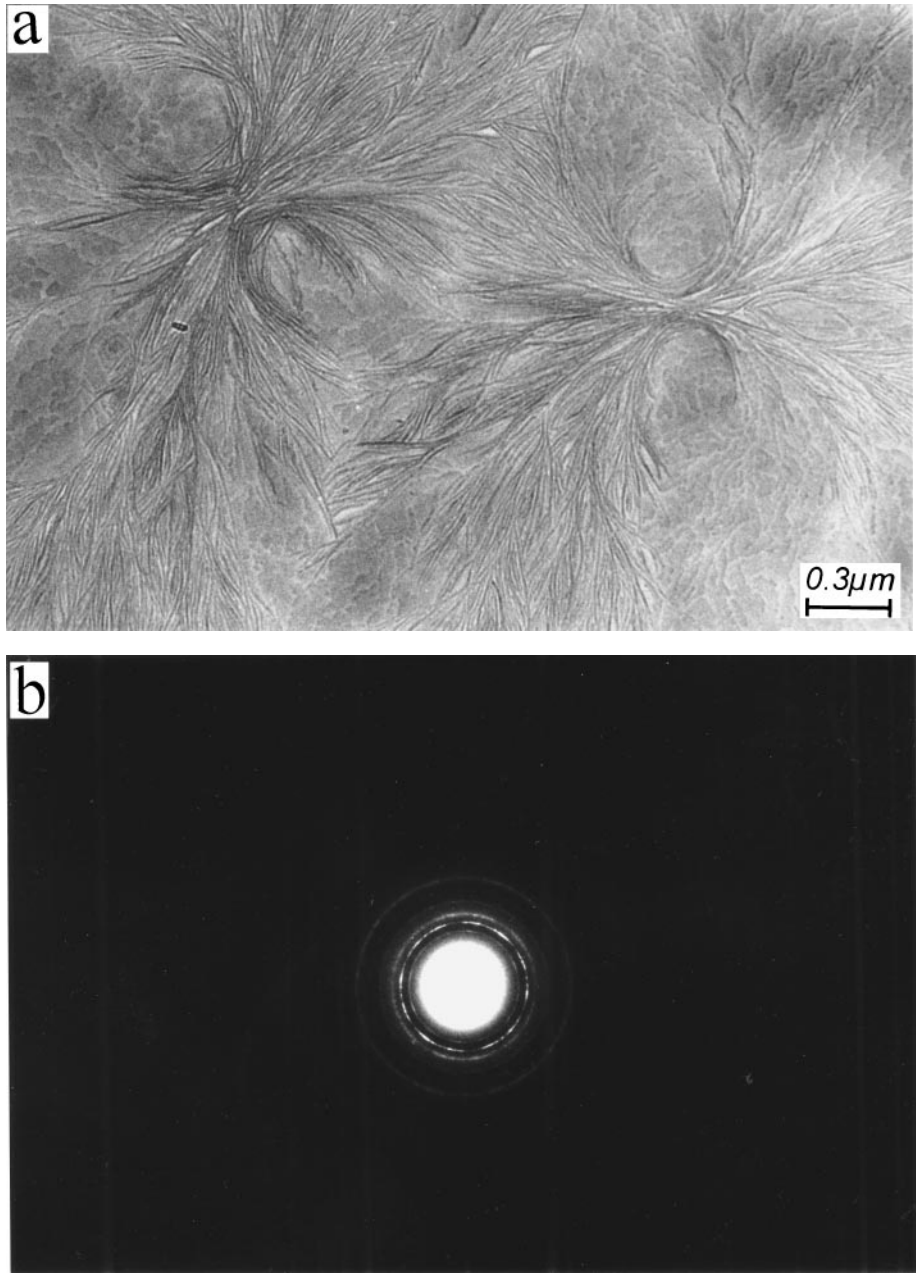

Figure 2 (a) BF electron micrograph and (b) electron diffraction pattern of iPS cold-crystallized isothermally at 160°C for 12 hours.

can be seen that the spherulitic structures consisting of closely packed edge-on lamellae are the main characteristic morphology for this crystallization temperature. A number of lamellar stacks grow from the central regions and continue outward by splaying and branching. Close inspection of the micrograph indicates, that between some thicker lamellae (especially for the outer lamellae) there exist some less perfect lamellae (probably consisting of some defective crystals, which may involve lattice defects, surface constrains and other irregularities) observed by a somewhat weaker phase (defocus) image contrast in the TEM. This morphology may be formed by the branching and splaying growth of individual dominant lamellae followed by infilling subsidiary growth [24]. The cause of splaying has been suggested by Keller *et al*. [25], resulting from uncrystallized molecular portions of cilia confined between lamellae. Here, the term "subsidiary lamellae" is used to describe these less perfect crystals which have not enough space to grow and are restricted within the framework of the dominant lamellae. Additionally, in the open regions of the film, flat-on crystals can be observed, particularly within the spherulitic "eyes" on either side of the nuclei. The contributions of these flat-on crystals to the electron diffraction (ED) pattern are the sharp reflection spots as can be seen in Fig. 2b.

It should be noted that the sample of Fig. 2 possesses triple melting peaks in the DSC heating scan. In order to investigate the origins of the multiple endotherms for iPS, the partial melting experiments are performed. Typically, the sample is thermally treated at a temperature just above the T_a, or $T_{m,1}$ for a short time (e.g., 1 min), and subsequently quenched to room temperature and then used for the TEM observations. If the multiple melting behavior results from the melting of different crystal populations, only the more stable (or thicker) lamellae, which have the higher melting temperature, are expected to be seen in the TEM micrographs. The

Figure 3 BF electron micrograph of an iPS sample as in Fig. 2, which was further treated at 190°C for 1 min and then quenched to room temperature.

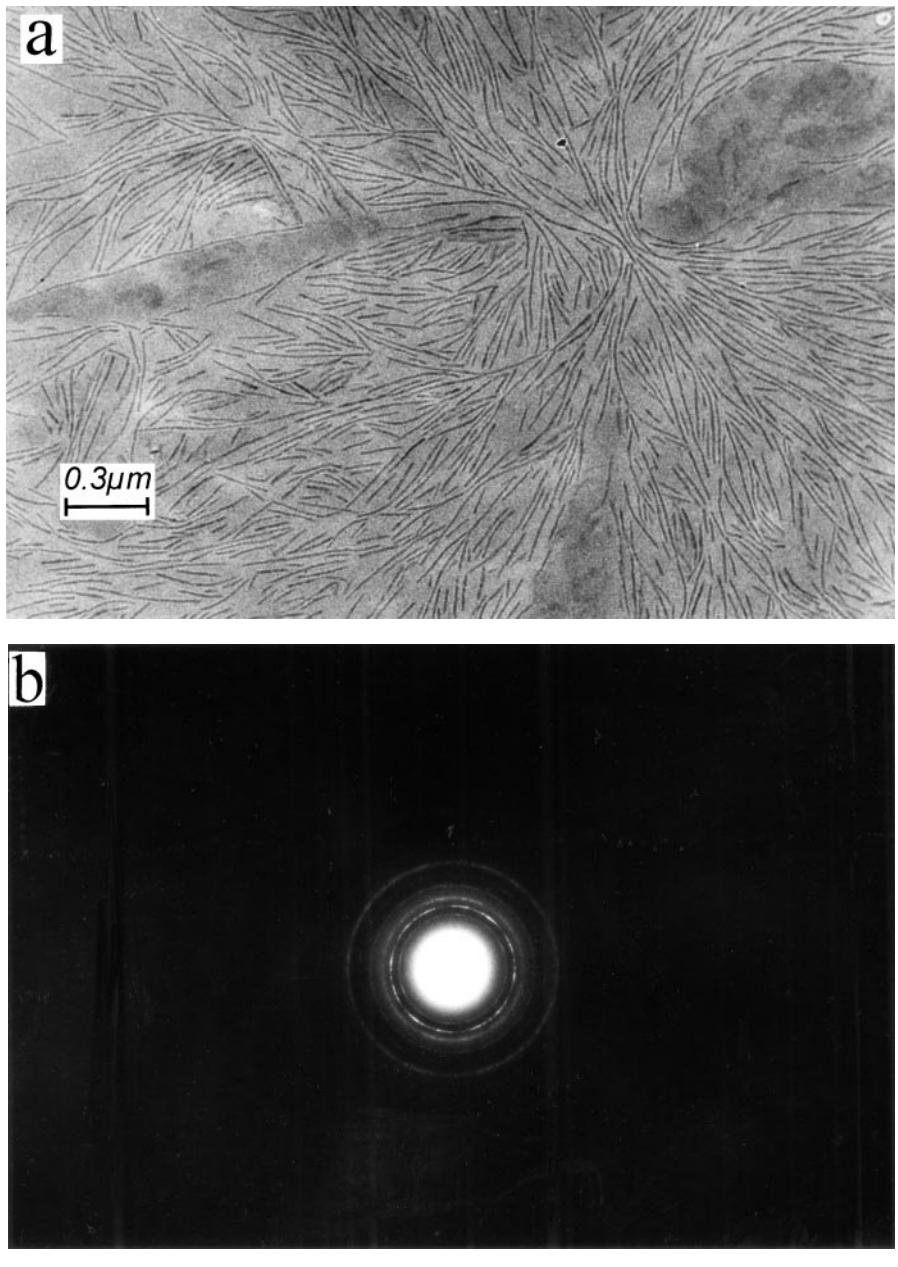

Figure 4 (a) BF electron micrograph and (b) electron diffraction pattern of an iPS sample as in Fig. 2 but partially melted at 212°C for 1 min.

two thermal treatment temperatures (190°C and 212°C) are chosen and indicated in Fig. 1. If the first endotherm (T_a) had originated from the melting of secondary crystals, as suggested by Challa *et al*., the secondary crystals are expected to be melted during the thermal treatment at 190°C. Fig. 3 shows the electron micrograph of the iPS sample as in Fig. 2, which was subsequently heat treated at 190°C for 1 min and quenched to room temperature. It can be seen, that there is no evident difference in the lamellar morphology from that observed in Fig. 2a. Therefore, it is likely that the first endothermic peak is not associated with the melting of subsidiary crystal populations. Concerning the origin of the first endothermic "annealing peak" for semicrystalline polymers, such as in PET, PPS, iPS and sPP (syndiotactic polypropyline), it has been pointed out in our other reports [18, 26, 27], that its occurrence is closely related to the enthalpy relaxation of a pseudo-crystalline interphase between the amorphous and crystalline phases, and no further discussion will be presented in this paper.

From Fig. 1 one can see, that the magnitude of $T_{m,1}$ is much smaller than that of $T_{m,2}$ for the iPS sample crystallized at 160°C. Therefore, when the initial crystalline sample undergoes partial melting treatment at a temperature just above the $T_{m,1}$ (such as 208°C, the peak temperature of $T_{c,re}$), no evident difference can be expected using the TEM technique. Hence, the partial melting experiments were conducted at a slightly higher temperature, here, at 212°C for 1 min, where fractions of the highest melting crystals ($T_{m,2}$) are involved in the melting process. The corresponding TEM micrograph and ED pattern are presented in Fig. 4. Only some more stable and thicker lamellae are left after the melting of the less perfect, thinner lamellae. Comparing the lamellar morphologies shown in Figs 2a and 4a, it is evident that firstly, after partial melting, the remaining lamellae almost have the same thickness as in the originally crystalline sample (Fig. 2a), but the TEM image contrast is improved; secondly, the densely and continuously packed lamellae become sparse and

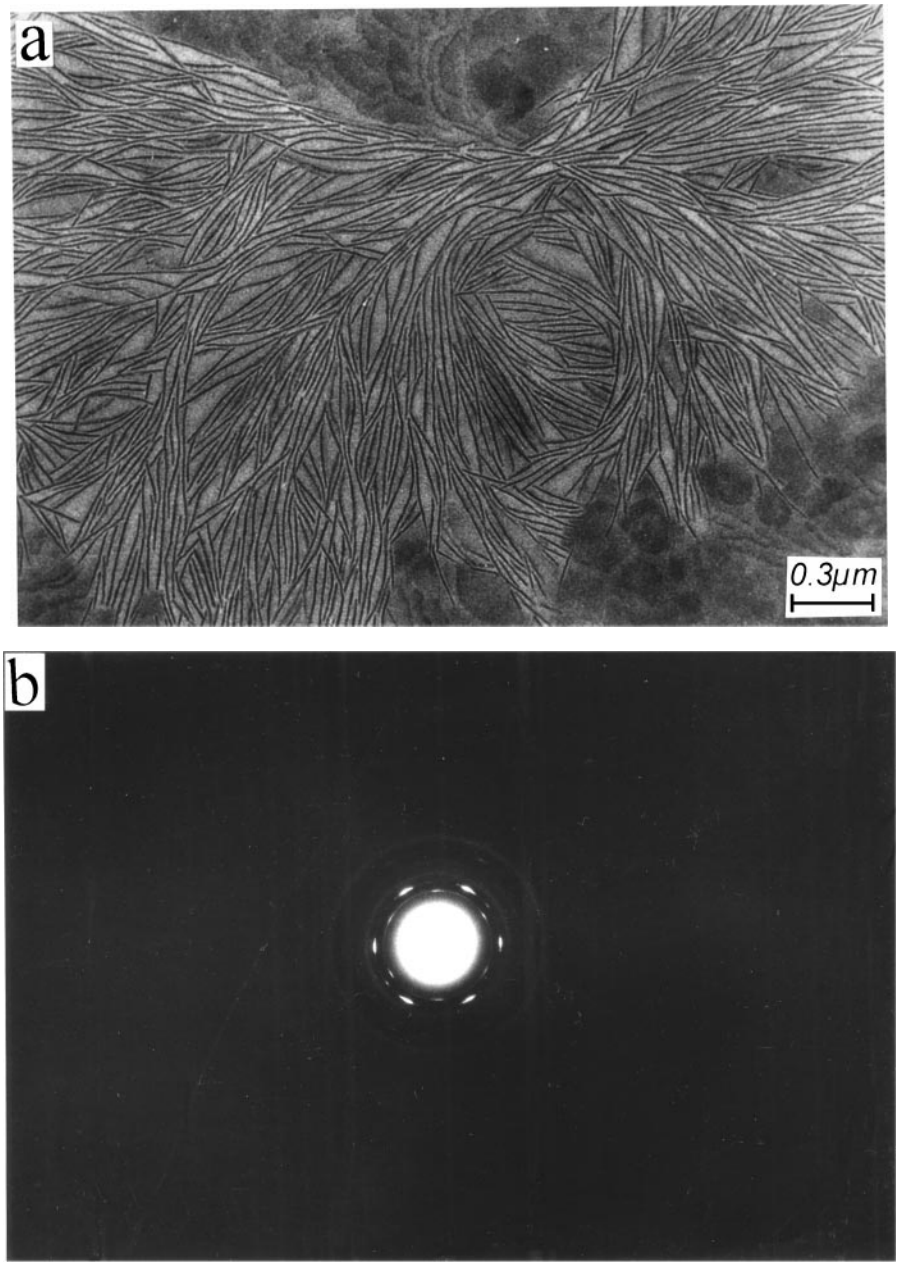

Figure 5 (a) BF electron micrograph and (b) electron diffraction pattern of an iPS sample as in Fig. 2 further treated at 212°C for 30 min.

discontinuous; thirdly, the electron diffraction intensity of the Debye Scherrer rings is significantly weakened after partial melting due to a loss in crystallinity (Fig. 4b).

Fig. 5 shows the TEM micrograph and ED pattern for the iPS sample further heat treated at 212°C for 30 min. One can see, that the "destroyed" (partially melted) stable lamellae (Fig. 4) are almost "renovated". The "renovated" lamellae are slightly thicker than those in Figs 2a and 4a. This may probably involve a solid-state thickening process by the consumption of less perfect lamellae during this longer retention. Also, the growth of single-crystal-like flat-on lamellae is now preferred. This can be seen from the open regions of Fig. 5a and the enhanced electron diffraction intensity of single-crystal-like diffraction spots (Fig. 5b). Therefore, just as Keller pointed out [28], during the heating process in the DSC, two competing processes are involved: melting and recrystallization. The predominance of the particular process depends on its rate compared with the heating rate: with slow heating rates, solid-state thickening is favored; while with fast heating rates, melting and subsequent recrystallization dominates [20].

The presence of the recrystallization exotherm just below the last melting peak is a direct indication, that the highest endotherm is partially originated from a recrystallized population originated in the heating process of the DSC. The recrystallization process may involve partial melting, rapid nucleation and recrystallization at the crystal surfaces (self seeding), which lead to more perfect or thicker crystals than the original ones. Due to the self seeding, the recrystallization is more rapid than ordinary isothermal crystallization at the same temperature. For iPS, it can be seen that the melting of subsidiary lamellae takes place just closely followed by the recrystallization process. As a consequence, the second melting endotherm ($T_{m,2}$) is, after the annealing and recrystallization procedure, shifted to somewhat higher temperature.

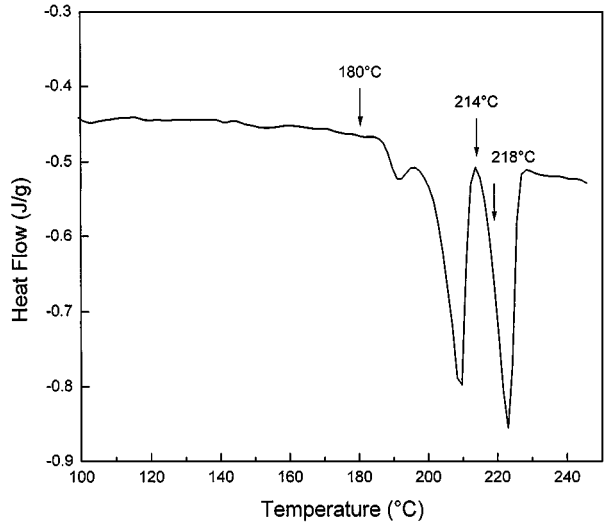

Figure 6 DSC thermogram of iPS cold-crystallized isothermally at 180°C for 10 hours. The heating rate is 10°C/min.

3.2. Investigations on iPS samples cold-crystallized isothermally at 180°C

The DSC thermogram and TEM micrograph of the iPS sample isothermally cold-crystallized at 180°C for 10 hours are shown in Figs 6 and 7, respectively. With the increase of crystallization temperature, the positions of T_a, $T_{m,1}$ and $T_{m,2}$ are shifted toward higher temperatures, and observed at about 192°C, 210°C (with heat of fusion, $\Delta H_m = 11.4$ J/g) and 223°C ($\Delta H_m = 13.5$ J/g), respectively. At this higher crystallization temperature (180°C), the recrystallization process is somewhat inhibited, therefore, the exothermic recrystallization peak, observed in the case of the sample crystallized at 160°C cannot be clearly seen. Furthermore, it can be seen, that for crystallization at 180°C the magnitude of the low-temperature melting peak ($T_{m,1}$) is strongly enhanced in comparison with the case of 160°C crystallized samples (compare Figs 1 and 6),

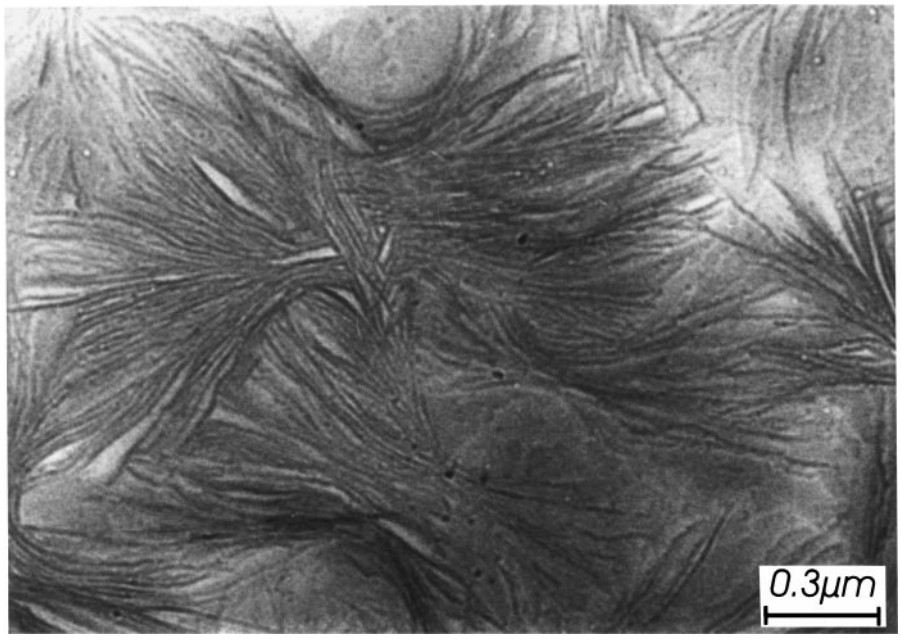

Figure 7 BF electron micrograph of iPS cold-crystallized isothermally at 180°C for 10 hours.

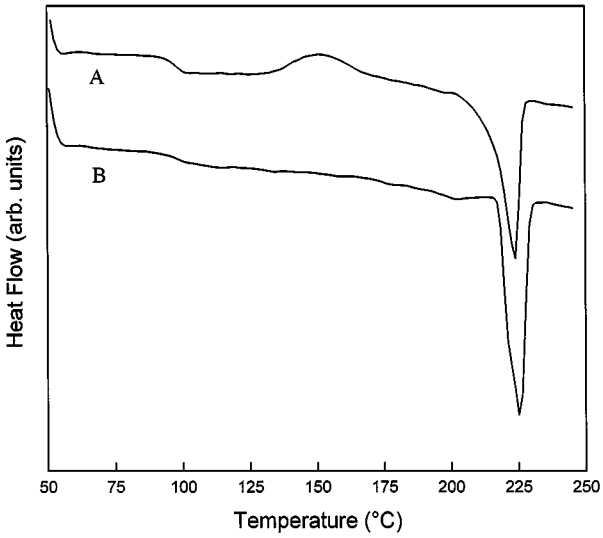

Figure 8 DSC thermograms of iPS samples as in Fig. 6, which were partially melted at 214°C for 1 min (curve A) and 60 min (curve B). The heating rate is 10°C/min.

and has become comparable with the high-temperature endotherm ($T_{m,2}$). Accordingly, the temperature (214°C) between the last two melting peaks is chosen as the approximate melting temperature of subsidiary crystals in the subsequent thermal treatment (indicated by the arrow in Fig. 8). From the bright field electron micrograph (Fig. 6) one can see, that the spherulites, which are formed at 180°C, mainly consist of closely packed stacks of parallel lamellae, and their outlines are less perfect and the overall sizes of spherulites are smaller than those formed at 160°C (see Fig. 2a). Close inspection of the micrograph also indicates, that some less perfect thinner lamellae are confined within the framework of the thicker ones.

Partial melting experiments performed on these iPS samples, cold-crystallized at 180°C for 10 hours, are depicted by DSC (Fig. 8) and TEM (Fig. 9) results. One initially crystalline sample was thermally treated at 214°C for 1 min, and subsequently quenched for DSC and TEM experiments (Fig. 8, curve A; Fig. 9a). The

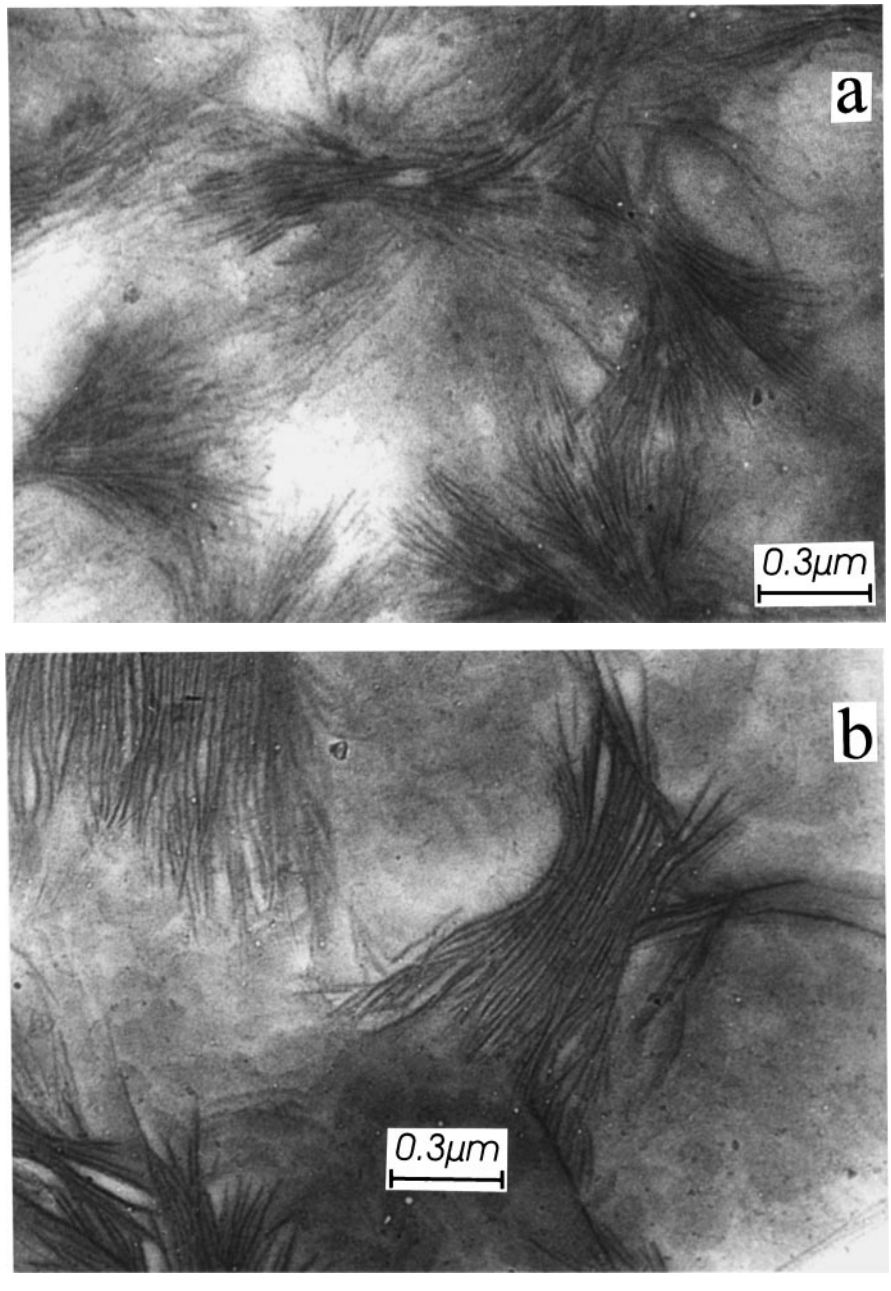

Figure 9 BF electron micrographs of iPS samples, which obtained the same thermal treatment as those in Fig. 8. (a) 1 min and (b) 60 min.

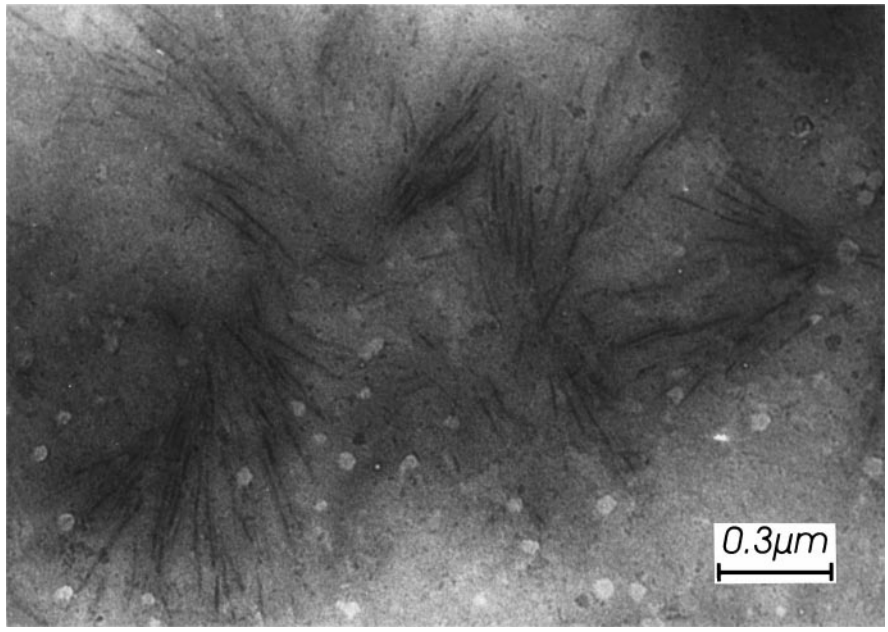

Figure 10 BF electron micrograph of iPS sample cold-crystallized isothermally at 180°C for 10 hours and then partially melted at 218°C for 1 min.

other one was held at 214°C for 60 min and quenched for subsequent measurements (Fig. 8, curve B; Fig. 9b). The heat flow signals in both DSC scans were normalized to the unit mass of the sample. The curves have been shifted vertically for the sake of clarity. From the partial melting experiments (Fig. 8) one can see, that after the retention at 214°C for 1 min, the low-temperature melting peak ($T_{m,1}$), which is probably associated with the subsidiary lamellae, disappears, and the melted secondary crystals recrystallize during the heating process in the DSC. Therefore, a broad exotherm can be seen at about 150°C on the DSC curve (Fig. 8, curve A). Consequently, the reorganized crystals melt at a slightly higher temperature (224.0°C) than the originally crystalline sample (223.0°C). After the retention at 214°C for 60 min, the melted subsidiary crystals have enough time to reorganize into more stable crystals, and therefore melt at an even higher temperature (225.2°C) with a larger heat of fusion (25.8 J/g) than in the case of 214°C for 1 min heat treated sample (22.3 J/g). In addition, a very weak endotherm can still be observed at about 202°C in curve B. It probably indicates that, the thinner lamellae are not completely melted after the partial melting at 214°C.

After the heat treatment at 214°C for 1 min and 60 min and the subsequent quenching, the samples only exhibit the high endothermic peak in the DSC heating scan. These changes in the thermal analysis can also be reflected by the morphological features from TEM observations. Fig. 9 presents the corresponding TEM images for the iPS samples with the same thermal history as in the DSC experiments (Fig. 8). Some thinner lamellae disappeared, while the thicker lamellae maintained but with poor contrast. These results indicate, that two populations of lamellar crystals exist before the heating process in the DSC. When the originally crystalline sample is heated in the DSC, the one lamellar population melts first due to its lower stability; the remaining stable lamellae will melt at a higher temperature. During this heating process, the melted subsidiary crystals might reorganize, to a lesser extent, into more stable lamellae. Therefore, the TEM observations have provided the evidence and proved the speculation that the low-temperature endotherm is ascribed to the melting of an unstable subsidiary crystal population between the more stable dominant ones. It is still unclear, and will be the subject of further investigations, from which reasons the two crystal populations result and what the precise difference is between the corresponding crystals. When further increasing the temperature in the partial melting experiments, for example, to 218°C for 1 min, the similar phenomenon as in the case of 160°C crystallized and at 212°C heat treated samples (Fig. 4a) is observed (Fig. 10). Most of the stable lamellae are melted and only a small amount of them remain. Evidently, the high-temperature endotherm is originated from the originally present stable dominant crystals, and to a less extent from the melting of the recrystallized population (which is not the representative amount of crystals in the material) formed during thermal scanning.

4. Conclusions

The triple melting endotherms of iPS cold-crystallized isothermally at two different temperatures (160°C and 180°C) are studied using DSC and TEM. Combining the morphological and thermal analysis studies, the low-temperature endotherm is attributed to the melting of less perfect subsidiary crystals formed within the framework of dominant lamellae upon isothermal crystallization. The high-temperature endotherm is originated from the originally present stable dominant crystals, and to a less extent from the recrystallization of the molten population during thermal scanning.

By taking account of the above-mentioned results for iPS, a three-phase model involving a mobile amorphous phase, a constrained "pseudo-crystalline" interphase and a crystalline phase (consisting of subsidiary and dominant populations) is proposed in order to describe

the complex melting and relaxation behavior of iPS. In this suggested model, the three phases play different roles in the thermal behavior during heating scans in the DSC, in which the enthalpy relaxation mechanism, the dual lamellar stack mechanism, and the melting-recrystallization mechanism are involved. During heating, firstly, the amorphous phase undergoes the glassy transition relaxation; then, the constrained interphase (pseudo crystals) experiences the enthalpic relaxation process; after that, the melting of subsidiary crystals is followed; finally, the melting of the dominant crystals and/or the reorganized ones takes place.

Acknowledgements

We are grateful to the Alexander von Humboldt-Stiftung for granting a stipend to T.Liu and to the Fonds der Chemischen Industrie for their financial support.

References

1. D. J. BLUNDELL and B. N. OSBORN, *Polymer* **24** (1983) 953.
2. D. J. BLUNDELL, *ibid.* **28** (1987) 2248.
3. P. CEBE and S. D. HONG, *ibid.* **27** (1986) 1183.
4. Y. LEE and R. S. PORTER, *Macromolecules* **20** (1987) 1336.
5. Y. LEE, R. S. PORTER and J. S. LIN, *ibid.* **22** (1989) 1756.
6. S. S. CHANG, *Polym. Commun.* **29** (1988) 138.
7. M. P. LATTIMER, J. K. HOBBS, M. J. HILL and P. J. BARHAM, *Polymer* **33** (1992) 3971.
8. R. K. VERMA, H. MARAND and B. S. HSIAO, *Macromolecules* **29** (1996) 7767.
9. B. S. HSIAO, K. H. GARDNER, D. Q. WU and B. CHU, *Polymer* **34** (1993) 3996.
10. K. N. KRÜGER and H. G. ZACHMANN, *Macromolecules* **26** (1993) 5205.
11. D. C. BASSETT, R. H. OLLEY and I. A. M. RAHEIL, *Polymer* **29** (1988) 1745.
12. S. Z. D. CHENG, M. Y. CAO and B. WUNDERLICH, *Macromolecules* **19** (1986) 1868.
13. H. MARAND and A. PRASAD, *ibid.* **25** (1992) 1731.
14. V. VELIKOV and H. MARAND, *Bull. Am. Phys. Soc*. **39** (1994) 569.
15. X. L. JI, W. J. ZHANG and Z. W. WU, *J. Polym. Sci. Phys. Edn.* **35** (1997) 431.
16. X. L. JI, D. H. YU, W. J. ZHANG and Z. W. WU, *Polymer* **38** (1997) 3501.
17. J. P. BELL and T. MURAYAMA, *J. Polym. Sci., Part A(2)* **7** (1969) 1059.
18. M. BONNET, K.-D. ROGAUSCH and J. PETERMANN, *Colloid Polym. Sci.* **277** (1999) 513.
19. R. K. VERMA and B. S. HSIAO, *Trends Polym. Sci*. **4** (1996) 312.
20. J. PETERMANN and R. M. GOHIL, *J. Macromol. Sci. Phys.* **B16**(2) (1979) 177.
21. J. BOON, G. CHALLA and D. W. VAN KREVELEN, *J. Polym. Sci., Part A(2)* **6** (1968) 1791.
22. P. J. LEMSTRA, T. KOOISTRA and G. CHALLA, *ibid.* **10** (1972) 823.
23. P. J. LEMSTRA, A. J. SCHOUTEN and G. CHALLA, *J. Polym. Sci. Phys. Edn.* **12** (1974) 1565.
24. D. C. BASSETT and A. S. VAUGHAN, *Polymer* **26** (1985) 717.
25. D. C. BASSETT, S. MITSUHASHI and A. KELLER, *J. Polym. Sci. A* **1** (1963) 73.
26. T. X. LIU and J. PETERMANN, Report for the Alexander von Humboldt Foundation, Nov. 1999.
27. M. STRANZ, Diploma thesis, Dortmund, Jan. 2000.
28. A. KELLER, *Repts. Progr. Phys.* **31**(Part 2) (1968) 623.

Received 17 January
and accepted 22 February 2000